NATIONAL ADVISORY COMMITTEE
FOR AERONAUTICS

TECHNICAL NOTE 2712

FLOW CHARACTERISTICS OVER A LIFTING WEDGE OF FINITE

ASPECT RATIO WITH ATTACHED AND DETACHED SHOCK

WAVES AT A MACH NUMBER OF 1.40

By John H. Hilton, Jr.

Langley Aeronautical Laboratory
Langley Field, Va.

NACA

Washington

June 1952

IV

NATIONAL ADVISORY COMMITTEE FOR AERONAUTICS

TECHNICAL NOTE 2712

FLOW CHARACTERISTICS OVER A LIFTING WEDGE OF FINITE

ASPECT RATIO WITH ATTACHED AND DETACHED SHOCK

WAVES AT A MACH NUMBER OF 1.40

By John H. Hilton, Jr.

SUMMARY

A series of schlieren photographs and pressure distributions are presented which show the effects of transition from an attached to a detached shock at the leading edge of a finite-span, 8.2° wedge as the angle of attack is increased. These data were obtained in the Langley 4- by 4-foot supersonic tunnel at a Mach number of 1.40.

INTRODUCTION

A knowledge of the mixed subsonic and supersonic flow region that exists near the leading edge of a wing when the bow shock is detached is of importance in the design of supersonic aircraft. The theoretical calculations (refs. 1 to 10) and experimental investigations (refs. 11 to 18) which have been conducted appear to be restricted to the study of detached shocks on models at zero angle of attack. References 14, 16, and 18, in particular, trace the transition from a detached to an attache shock as the Mach number is increased.

Data pertaining to the transition from an attached to a detached shock as the angle of attack is increased were obtained in the Langley 4- by 4-foot supersonic tunnel during the course of an investigation which had other primary objectives. The tests were made at a Mach number of 1.40 with a wedge airfoil having an 8.2° apex angle. The model, which did not span the test section, was 16 inches wide and had a chord of 4.9 inches. A series of schlieren photographs and pressure distributions along the midspan of the forward portion of the model were obtained through an angle-of-attack range from 0° to 11° in 1° increments. The resulting pressure data have been integrated to obtain section aerodynamic coefficients at midspan and are presented with the schlieren photographs to supplement existing data on the effects of shock detachment. Some pressure data were measured in the three-dimensional flow field of the wing tips and are applicable only to wedges of the same aspect ratio as the test model.

SYMBOLS

c_n section normal-force coefficient, n/qc_w

c_c section chord-force coefficient (base pressure assumed equal to free-stream static pressure), c/qc_w

n section normal force, lb

c section chord force (base pressure assumed equal to free-stream static pressure), lb

c_w wedge chord, distance from leading edge to station of maximum thickness, ft

q free-stream dynamic pressure, lb/sq ft

P pressure coefficient, $\dfrac{p_l - p}{q}$

p_l local static pressure, lb/sq ft

p free-stream static pressure, lb/sq ft

α angle of attack of wedge-chord line, deg

M Mach number

Subscripts:

s surface

t theoretical local value

MODEL AND APPARATUS

The tests were conducted in the Langley 4- by 4-foot supersonic tunnel which is a rectangular, closed-throat, single-return wind tunnel having a design Mach number range from 1.2 to 2.2. The test-section Mach number is varied by deflecting the top and bottom walls of the supersonic nozzle against interchangeable templets which have been designed to produce uniform flow in the test section. The nozzle walls were set for a Mach number of 1.40 for these tests. At this Mach number, the test section has a width of 4.5 feet and a height of 4.4 feet. The

Mach number variation in the test section is ±0.01 and the maximum flow irregularity about 1/4°.

The model (fig. 1) was constructed of mild steel and was designed primarily for simplicity of fabrication and installation. The model had a modified diamond airfoil section. The wedge formed by the portion of the airfoil forward of the point of maximum thickness had an apex angle of 8.2°, a chord of 4.9 inches, and a span of 16 inches (aspect ratio of 3.3). A longitudinal row of six orifices was located at midspan on both the upper and lower surfaces. The leading-edge thickness was approximately 0.002 inch.

The model was sting-mounted and the angle of attack was varied by means of an external bell-crank mechanism (fig. 2). Figure 3 shows the model mounted in the tunnel.

TESTS

The tests were conducted at a Mach number of 1.40 and at the following stagnation conditions:

Pressure, atm 0.25
Temperature, °F 110
Dew point, °F . . . . -16 to -27

The dynamic pressure was about 229 pounds per square foot and the Reynolds number based on a wedge chord of 4.9 inches was approximately 437,000.

Simultaneous pressure measurements and schlieren photographs were obtained for an angle-of-attack range of 0° to 11° in 1° increments. An additional schlieren photograph was taken at an angle of attack of 12°, a condition for which the tunnel was choked at the rear of the model.

RESULTS AND DISCUSSION

A series of schlieren photographs and pressure distributions are presented to illustrate the general characteristics of the flow over a wedge having attached and detached shocks. The pressure distributions are compared with shock-expansion theory and have been integrated to provide an interpretation of the data in terms of the section normal-force coefficient, section chord-force coefficient, and section center of pressure at midspan.

The schlieren photographs and pressure distributions (fig. 4) are presented for an angle-of-attack range from 0° to 11°. The inserts shown on the schlieren photographs are explained in the schematic drawing in figure 5. (M_t is calculated by assuming a straight leading-edge shock.)

The flow behind the attached shock is completely supersonic at mid-span for an angle of attack of 0° (fig. 4(a)). As the angle of attack is increased, the Mach number increases on the upper surface and decreases on the lower surface until, at an angle of attack of about 5° (fig. 4(f)), the flow on the lower surface becomes subsonic. The maximum theoretical flow deflection angle occurs at an angle of attack of 5.3° (total stream deflection angle of 9.4°). At angles of attack above 5°, the shock wave gradually detaches and moves forward of the leading edge (figs. 4(g) to 4(l)).

Schlieren Photographs and Pressure Distributions

Attached shock.- The attached shock is slightly curved at the leading edge for all angles of attack, as can be seen in the schlieren photographs in figures 4(a) to 4(f) and 6. This curvature is probably due partly to the development of the boundary-layer displacement thick-ness in the vicinity of the leading edge (ref. 19) and partly to blunt-ness of the leading edge. An attached shock exists on both the upper and lower surfaces at angles of attack of 4° and 5°, even though the upper surface is alined with the free stream at 4° angle of attack and is at a negative (expansion) angle with respect to the free stream at 5° angle of attack. These shock waves may be due to flow conditions at the tips. If so, the shock would not extend across the entire span but would be located in the vicinity of the wing tips.

The pressure distributions in figures 4(a) to 4(f) indicate that the regions of two-dimensional flow (regions not affected by tip flow) are well-described by shock-expansion theory. The slight departure of the experimental pressures from the straight-line distribution associ-ated with a flat surface may be caused by model or air-stream irregu-larities. The effect of the build-up of the boundary-layer displacement thickness on the pressures at and behind the first orifice is very small. In the three-dimensional field, an accurate theoretical solution is not available. The approximate method of reference 20 was used, how-ever, to estimate the effects of the tips for angles of attack of 3° and 4° (figs. 4(d) and 4(e)).

Detached shock.- The bow wave detaches, theoretically, at an angle of attack of approximately 5.3° and moves ahead of the leading edge as the angle of attack is further increased (figs. 4(g) to 4(l)). The

transition from attached to detached shock is a progressive phenomenon as shown in the schlieren photographs. In the flow field behind the shock a small region of large density gradient exists near the leading edge of the upper surface and is followed by an attached, oblique shock (fig. 4(h)). In order to present a clearer illustration of this region, an additional schlieren photograph, taken at an angle of attack of 12°, is shown as figure 7. The density-gradient field is reversed in this photograph because of a new position of the knife edge. (The light region along the lower surface is due to diffraction effects.)

At an angle of attack of 8° (fig. 4(i)) the boundary layer on the upper surface appears to separate near the last orifice. The separation, which moves upstream with increased angle of attack, may be due, in part, to positive pressure transmitted forward through the boundary layer. This adverse pressure may be caused by a compression of the flow on the model support and, at high angles of attack, by a tunnel choking shock located near the trailing edge of the model.

Pressure coefficients were calculated by means of the two-dimensional shock-expansion theory for the upper surface for all angles of attack beyond the angle of attack of shock detachment (figs. 4(g) to 4(l)). The presence of the bow wave was neglected for these calculations. The theory is in good agreement with the experimental pressures through part of the range; this agreement, however, may be due to compensating effects of the complex flow field at the leading edge. At the higher angles of attack, the experimental pressures near the rear of the upper surface become more positive, possibly because of the adverse pressures transmitted through the boundary layer.

Aerodynamic Coefficients

The experimental and theoretical values for the section normal-force coefficient, section chord-force coefficient, and section center of pressure at midspan are shown in figure 8 and the corresponding aerodynamic coefficients of the individual surfaces of the wedge are presented in figure 9. The base pressure was assumed to be equal to the free-stream static pressure. (The surface values have been defined as the contribution of the individual surfaces to the total coefficients.) In order to illustrate the transition from an expansion to a compression surface, the data of figure 9 have been replotted in terms of surface incidence angles (fig. 10). The sign convention for the aerodynamic coefficients has been arbitrarily defined as positive if the flow is compressed and negative if the flow is expanded. The theoretical values are given for angles of attack up to 5°. These values were obtained by neglecting three-dimensional effects and using the theory for two-dimensional flow. The agreement between the experimental and theoretical values of the aerodynamic coefficients is good. As can be seen from

these curves, the change from attached to detached shock is a gradual phenomenon resulting in no radical changes in the aerodynamic coefficients.

CONCLUDING REMARKS

A series of schlieren photographs, midspan pressure distributions, and aerodynamic coefficients have been presented for an 8.2° wedge of aspect ratio 3.3. The data, which were taken over an angle-of-attack range of 0° to 11° at a Mach number of 1.40, illustrate the general characteristics of supersonic flow over a wedge and show the effects of transition from an attached to a detached shock wave at the leading edge.

Langley Aeronautical Laboratory
    National Advisory Committee for Aeronautics
        Langley Field, Va., March 12, 1952

REFERENCES

1. Maccoll, J. W.: Investigation of Compressible Flow at Sonic Speeds. Theoretical Res. Rep. No. 7/46, Armament Res. Dept., British Ministry of Supply, Sept. 1946.

2. Drougge, Georg: The Flow around Conical Tips in the Upper Transsonic Range. Rep. No. 25, Aero. Res. Inst. of Sweden (Stockholm), 1948.

3. Guderley, K. Gottfried: Considerations of the Structure of Mixed Subsonic-Supersonic Flow Patterns. Tech. Rep. No. F-TR-2168-ND, Air Materiel Command, U.S. Air Force, Oct. 1947.

4. Lin, C. C., and Rubinov, S. I.: On the Flow behind Curved Shocks. Jour. Math. and Phys., vol. XXVII, no. 2, July 1948, pp. 105-129.

5. Dugundji, John: An Investigation of the Detached Shock in Front of a Body of Revolution. Jour. Aero. Sci., vol. 15, no. 12, Dec. 1948, pp. 699-705.

6. Busemann, Adolf: A Review of Analytical Methods for the Treatment of Flows with Detached Shocks. NACA TN 1858, 1949.

7. Wood, George P., and Gooderum, Paul B.: Method of Determining Initial Tangents of Contours of Flow Variables behind a Curved, Axially Symmetric Shock Wave. NACA TN 2411, 1951.

8. Guderley, Gottfried, and Yoshihara, Hideo: The Flow over a Wedge Profile at Mach Number One. Tech. Rep. No. 5783, ATI No. 57842, Air Materiel Command, U.S. Air Force, July 1949.

9. Vincenti, Walter G., and Wagoner, Cleo B.: Transonic Flow past a Wedge Profile with Detached Bow Wave - General Analytical Method and Final Calculated Results. NACA TN 2339, 1951.

10. Moeckel, W. E.: Approximate Method for Predicting Form and Location of Detached Shock Waves ahead of Plane or Axially Symmetric Bodies. NACA TN 1921, 1949.

11. Ladenburg, R., Van Voorhis, C. C., and Winckler, J.: Interferometric Study of Supersonic Phenomena. Part I: A Supersonic Air Jet at 60 LB/IN^2 Tank Pressure. NAVORD Rep. 69-46, Bur. Ordnance, Navy Dept., Apr. 17, 1946.

12. Heberle, Juergen W., Wood, George P., and Gooderum, Paul B.: Data on Shape and Location of Detached Shock Waves on Cones and Spheres. NACA TN 2000, 1950.

13. Pack, D. C.: Investigation of the Flow past Finite Wedges of
    20 Deg. and 40 Deg. Apex Angle at Subsonic and Supersonic Speeds,
    Using a Mach-Zehnder Interferometer. R. & M. No. 2321, British
    A.R.C., 1949.

14. Drougge, G.: A Method for the Continuous Variation of the Mach
    Number in a Supersonic Wind Tunnel and Some Experimental Results
    Obtained at Low Supersonic Speeds. Rep. No. 29, Aero. Res. Inst.
    of Sweden (Stockholm), 1949.

15. Gooderum, Paul B., and Wood, George P.: Density Fields around a
    Sphere at Mach Numbers 1.30 and 1.62. NACA TN 2173, 1950.

16. Liepmann, H. W., and Bryson, A. E., Jr.: Transonic Flow past Wedge
    Sections. Jour. Aero. Sci., vol. 17, no. 12, Dec. 1950,
    pp. 745-755.

17. Griffith, Wayland C.: Transonic Flow. Tech. Rep. II - 7, Princeton
    Univ., Dept. of Phys., Dec. 19, 1950.

18. Bryson, Arthur Earl, Jr.: An Experimental Investigation of Tran-
    sonic Flow past Two-Dimensional Wedge and Circular-Arc Sections
    Using a Mach-Zehnder Interferometer. NACA TN 2560, 1951.

19. Liepmann, Hans Wolfgang, Askenas, Harry, and Cole, Julian D.:
    Experiments in Transonic Flow. AF TR No. 5667, Air Materiel
    Command, Feb. 9, 1948.

20. Czarnecki, K. R., and Mueller, James N.: An Approximate Method of
    Calculating Pressures in the Tip Region of a Rectangular Wing of
    Circular-Arc Section at Supersonic Speeds. NACA TN 2211, 1950.
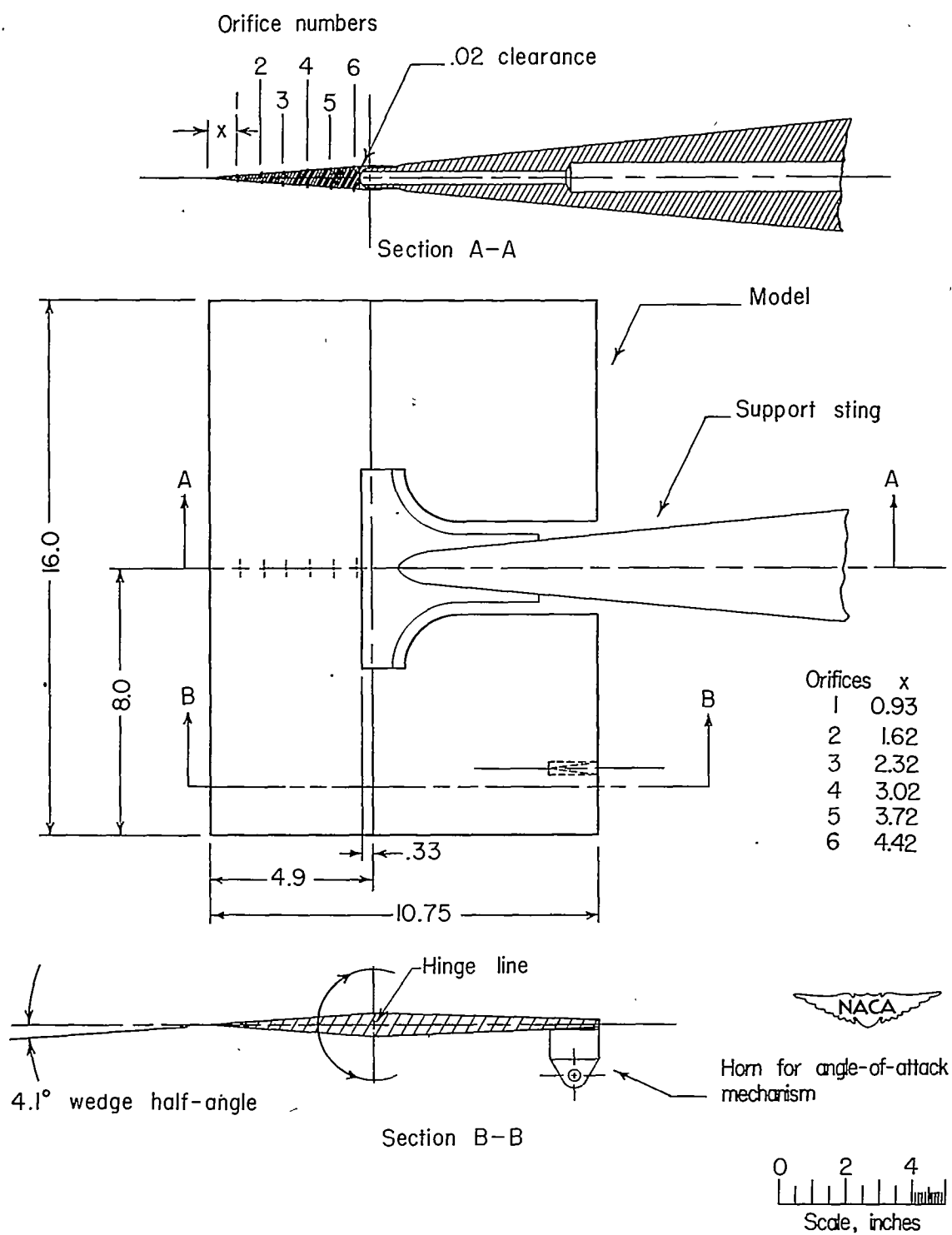
Orifice numbers

Section A-A

.02 clearance

Model

Support sting

A   A

B   B

Orifices	x
I	0.93
2	1.62
3	2.32
4	3.02
5	3.72
6	4.42

16.0

8.0

.33

4.9

10.75

Hinge line

4.1° wedge half-angle

NACA

Horn for angle-of-attack mechanism

Section B-B

0   2   4

Scale, inches

Figure 1.- Model and model-mounting arrangement.

Model

Bell-crank angle-of-attack mechanism

Support sting

Fixed support strut

NACA

L-67568
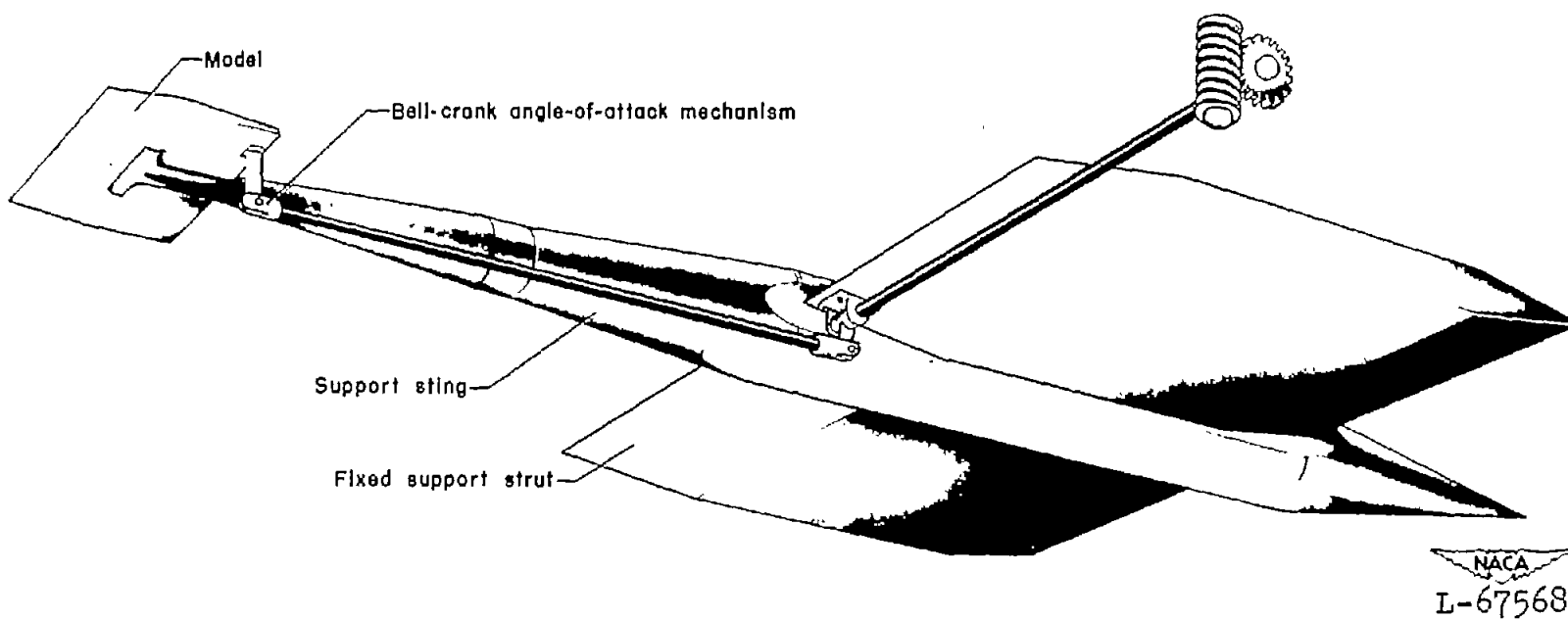
Figure 2.- Model installation in tunnel.
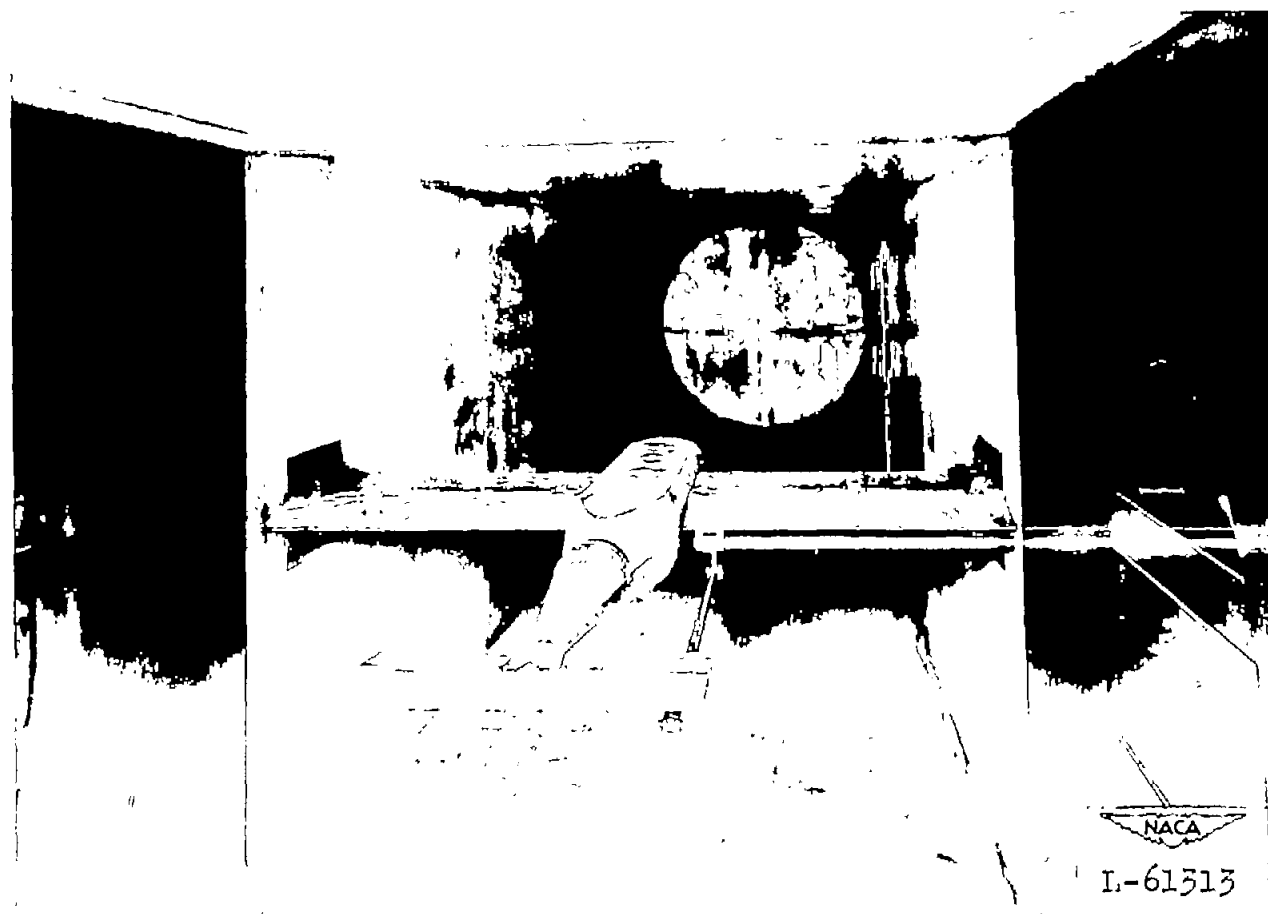
Figure 3.- Photograph of model mounted in Langley 4- by 4-foot supersonic tunnel.
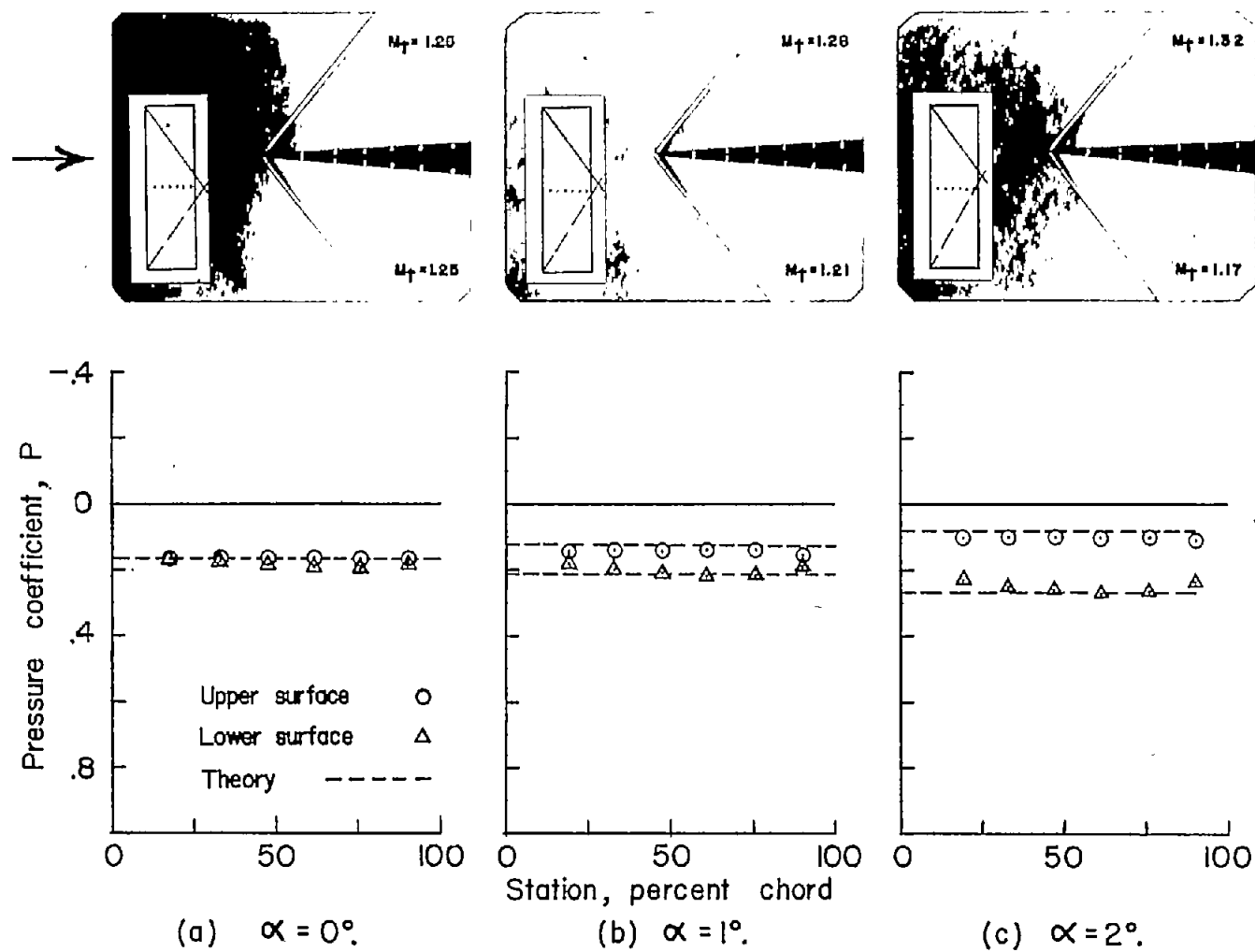
Figure 4.— Schlieren photographs and pressure distributions for an 8.2° wedge at a Mach number of 1.40. Theoretical distributions calculated by shock-expansion theory are also shown.

L-74373

(d) $\alpha = 3°$.   (e) $\alpha = 4°$.   (f) $\alpha = 5°$.

Figure 4.- Continued.

L-74374

(g) $\alpha = 6°$.

(h) $\alpha = 7°$.

(i) $\alpha = 8°$.
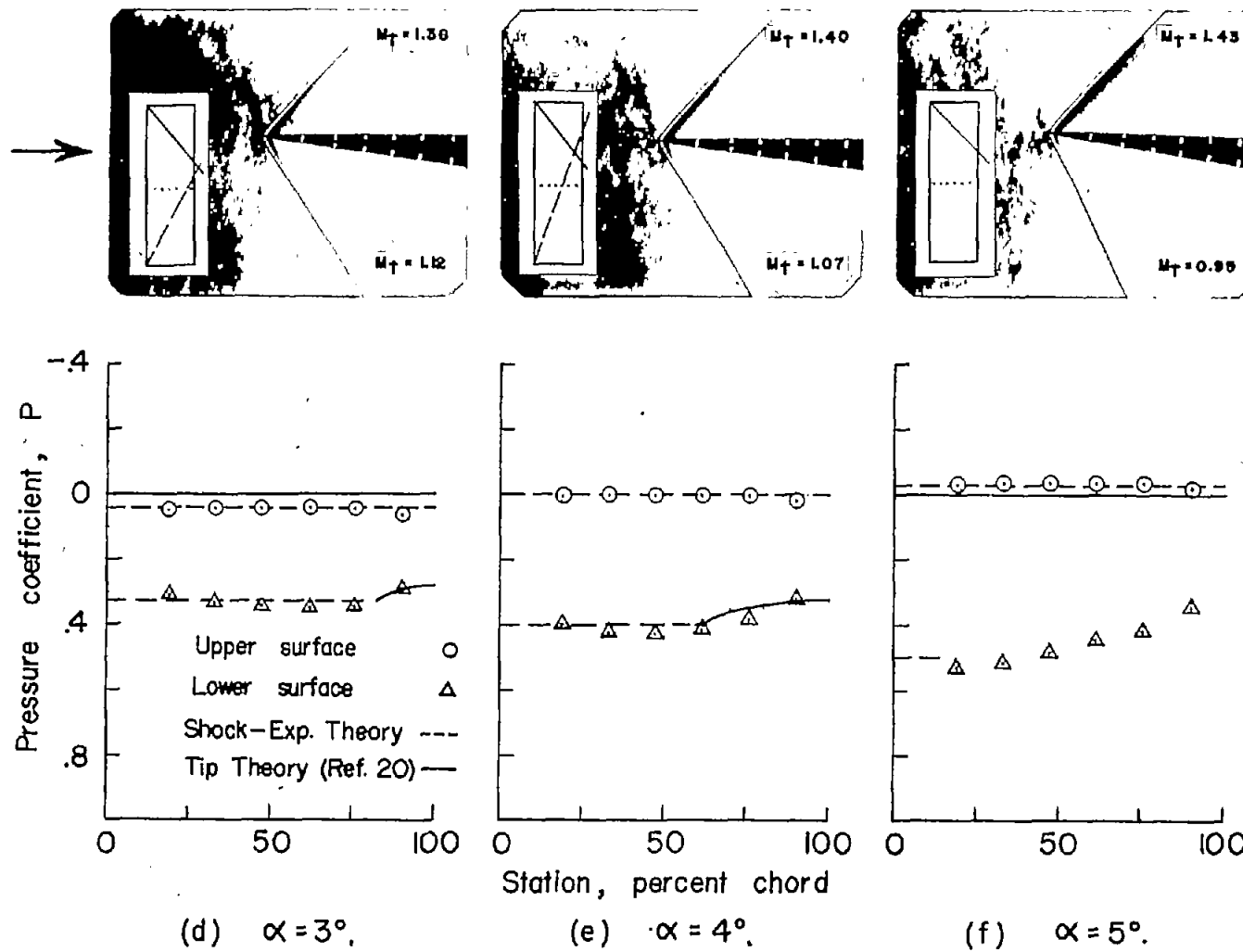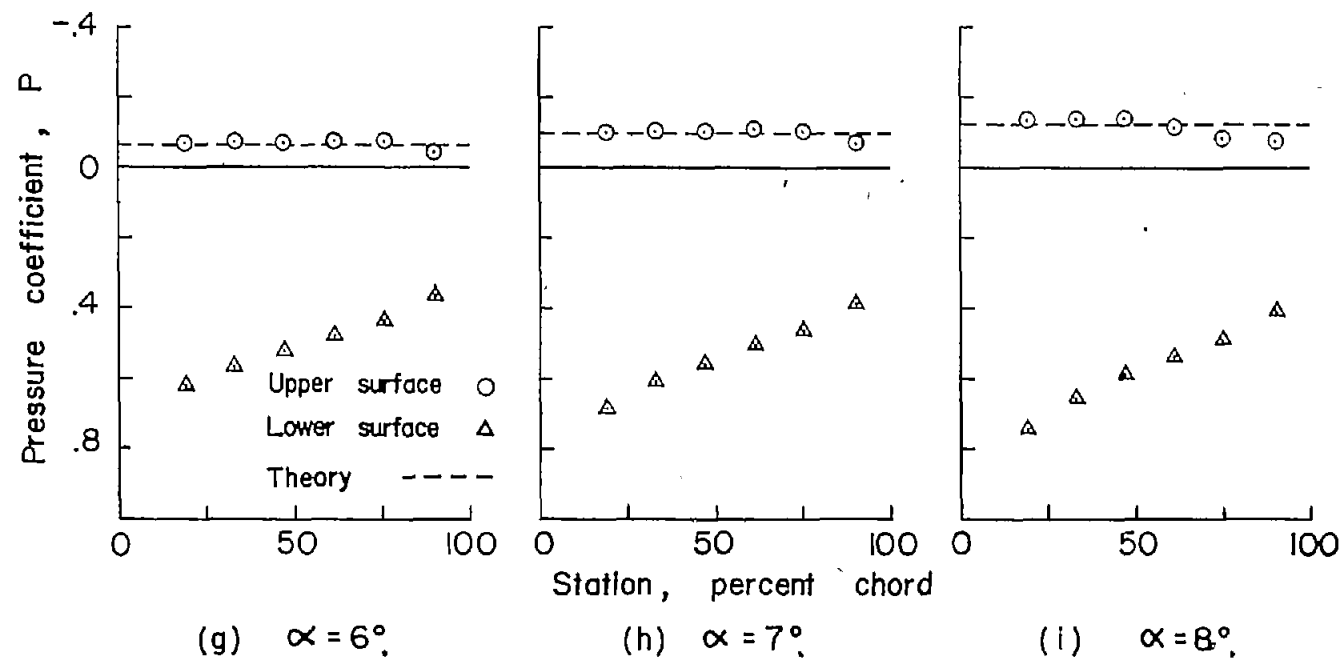
Figure 4.- Continued.

L-74375

Figure 4.- Concluded.

L-74376

Upper – surface Mach line

Wedge plan form

Theoretical surface
Mach numbers from
shock – expansion theory
$\alpha = 3°$

$M_f = 1.36$

Air flow

$M = 1.40$

Orifice locations

$M_f = 1.12$

Lower—surface Mach line

Orifice locations
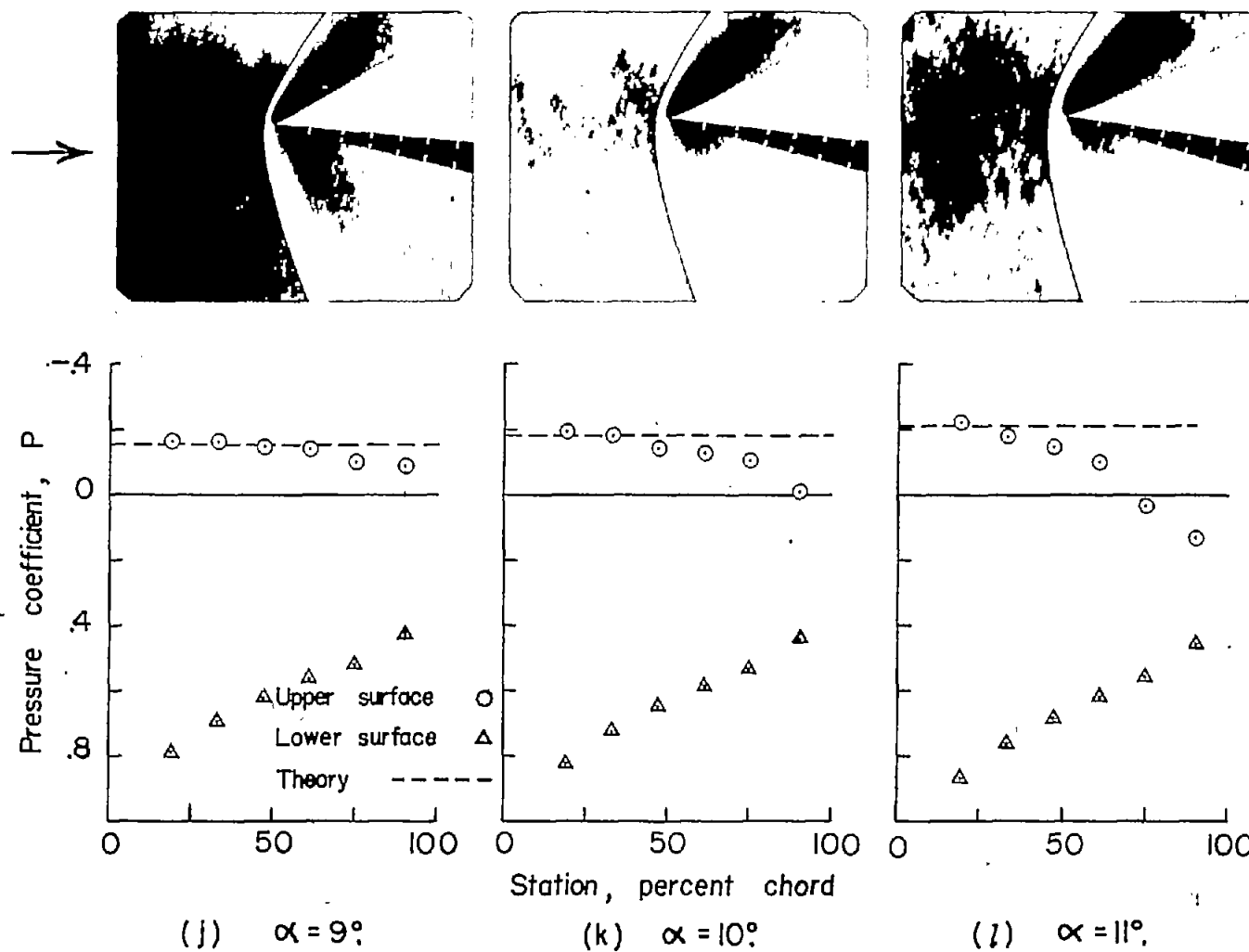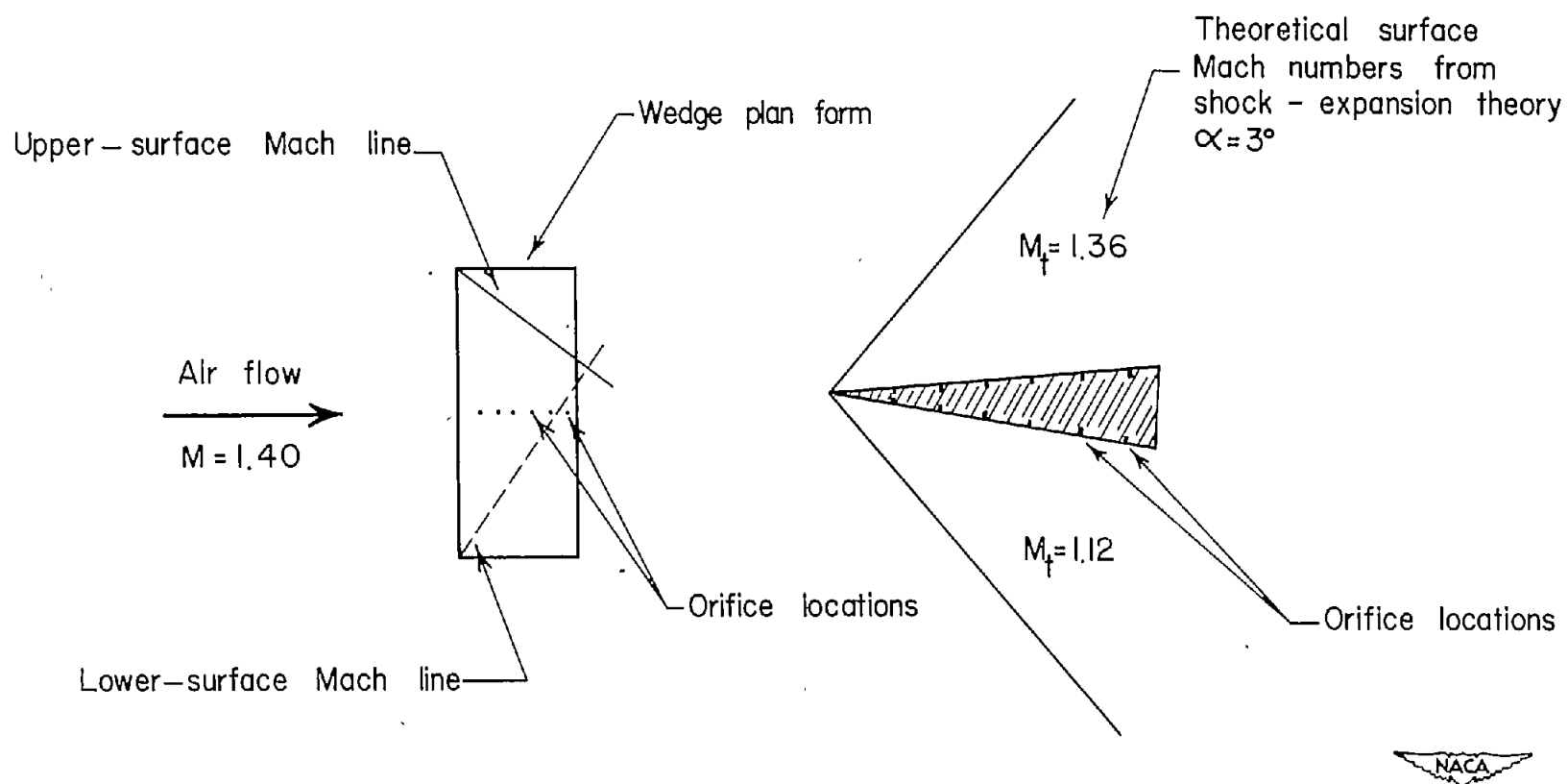
NACA

Figure 5.- Explanation of inserts on schlieren photographs.

(a) $\alpha = 0°$.

(b) $\alpha = 5°$.
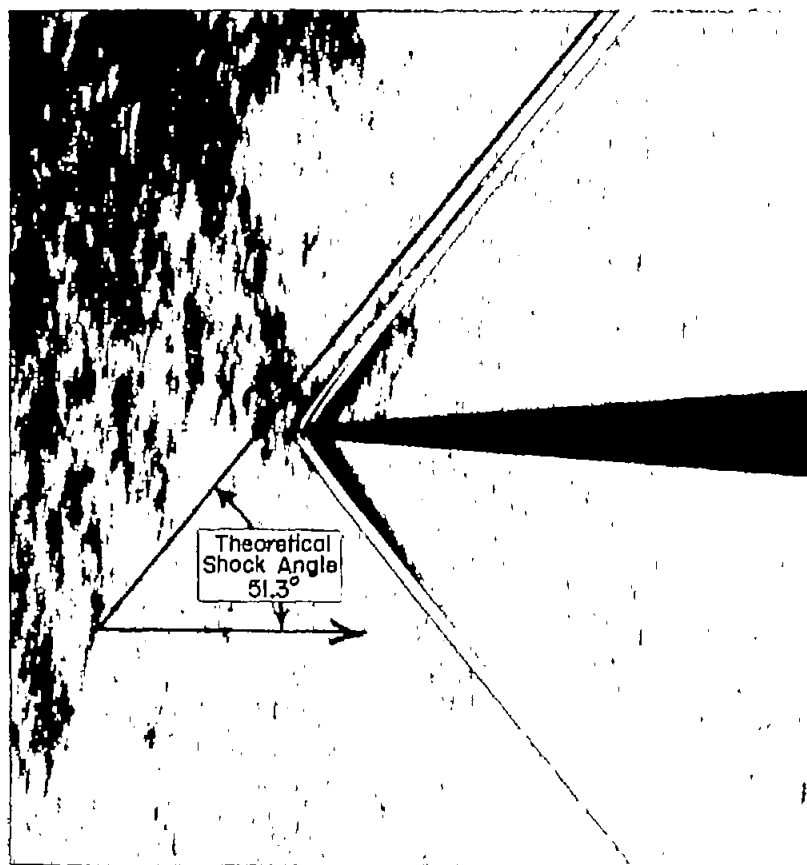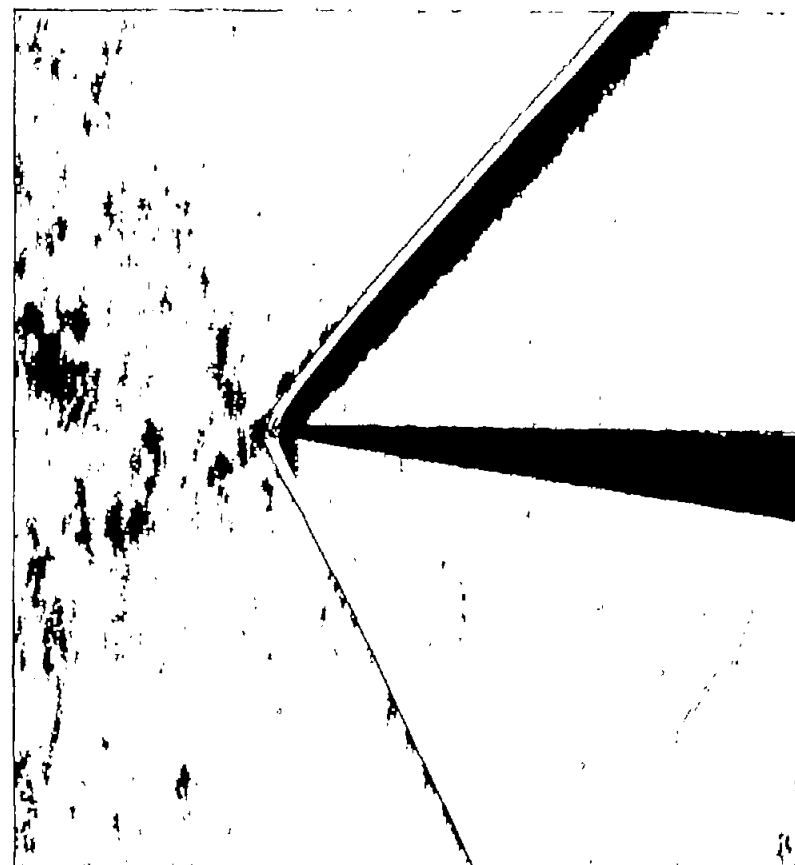
L-74377

Figure 6.- Shock formation at $\alpha = 0°$ and $\alpha = 5°$ for an 8.2° wedge.
M = 1.40.
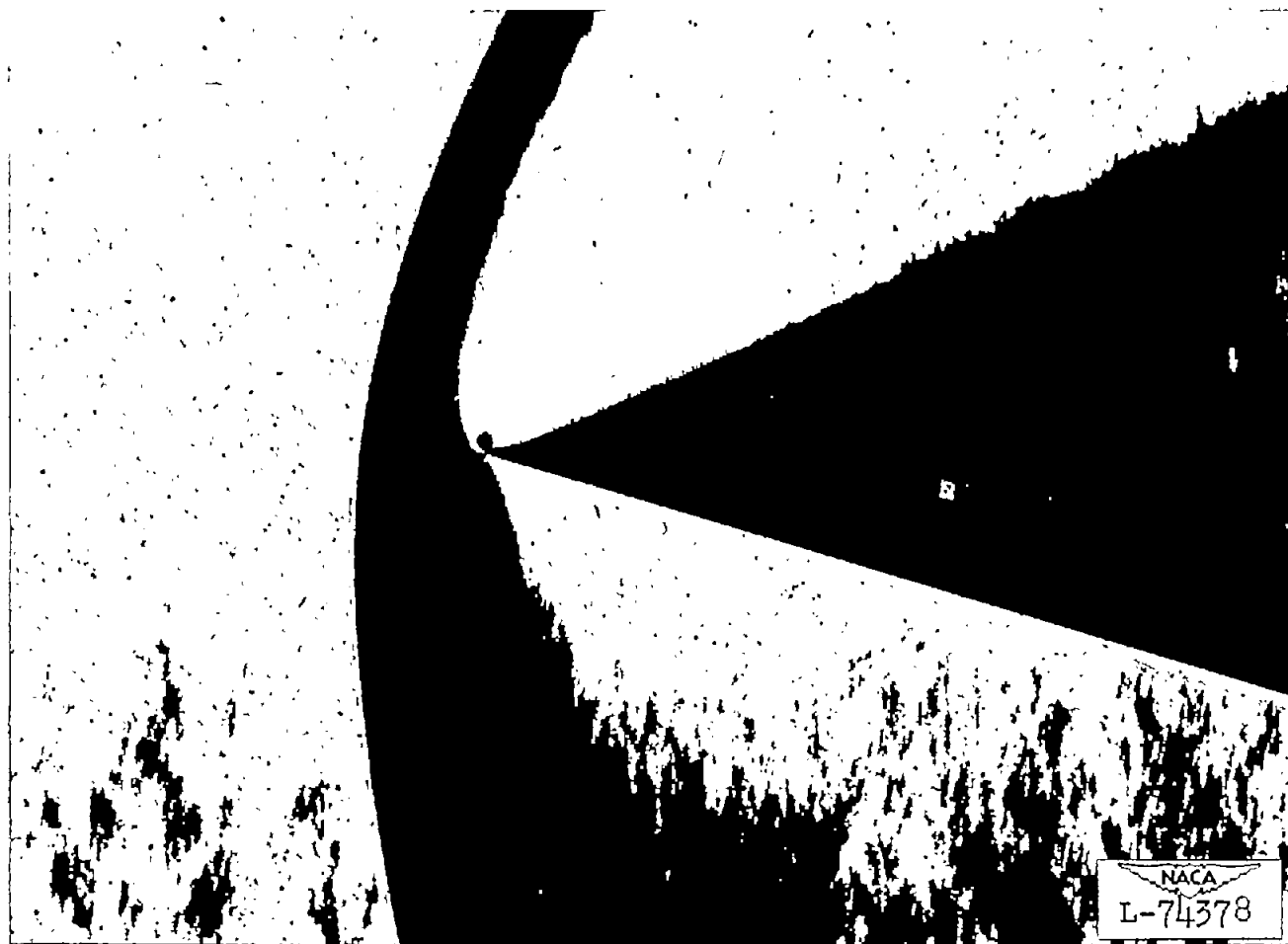
Figure 7.- Schlieren photograph of flow conditions at an angle of
attack of 12°.

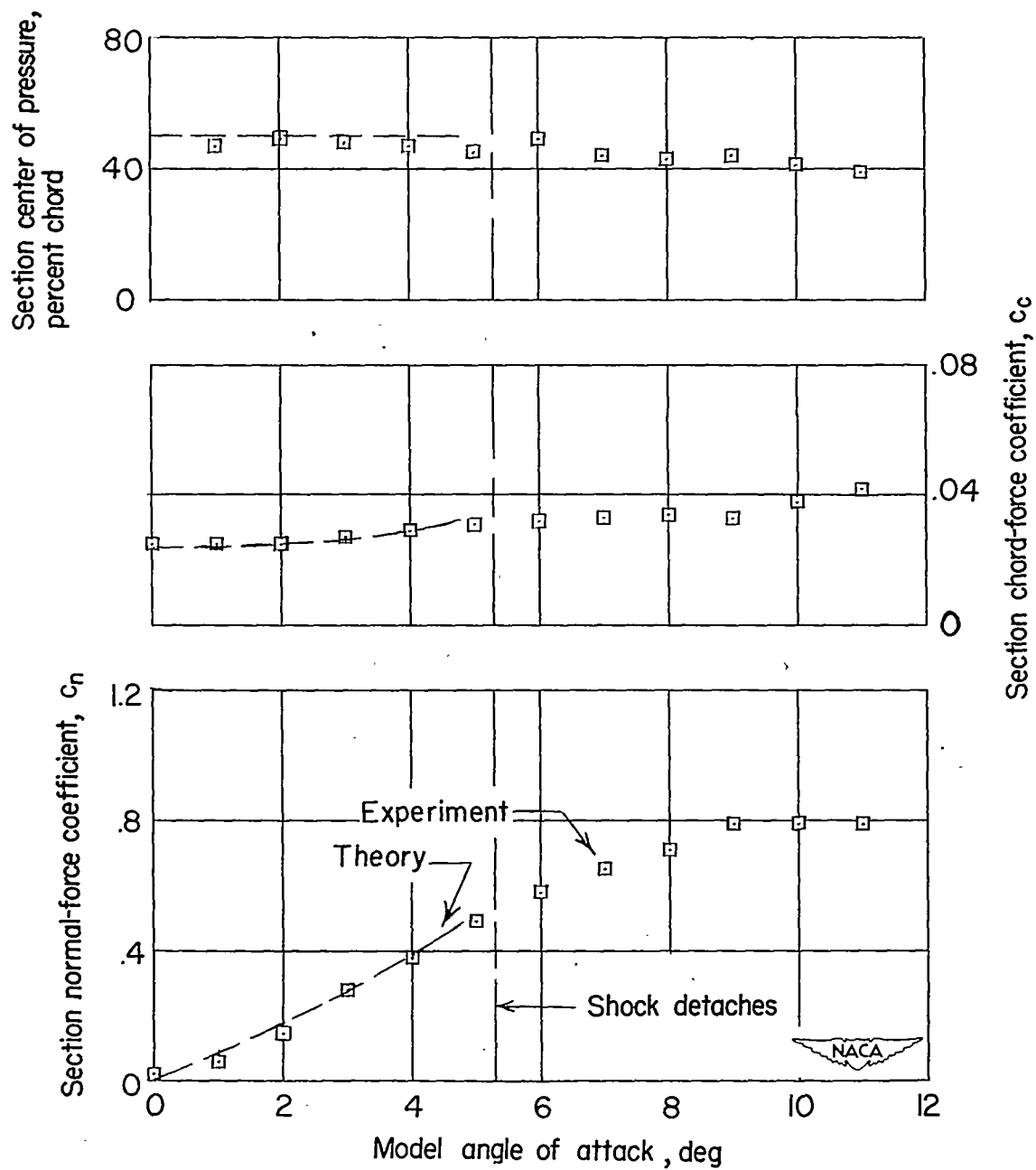Figure 8.- Aerodynamic characteristics at the midspan of an 8.2° wedge
of aspect ratio 3.3. M = 1.40. Base pressure assumed equal to free-
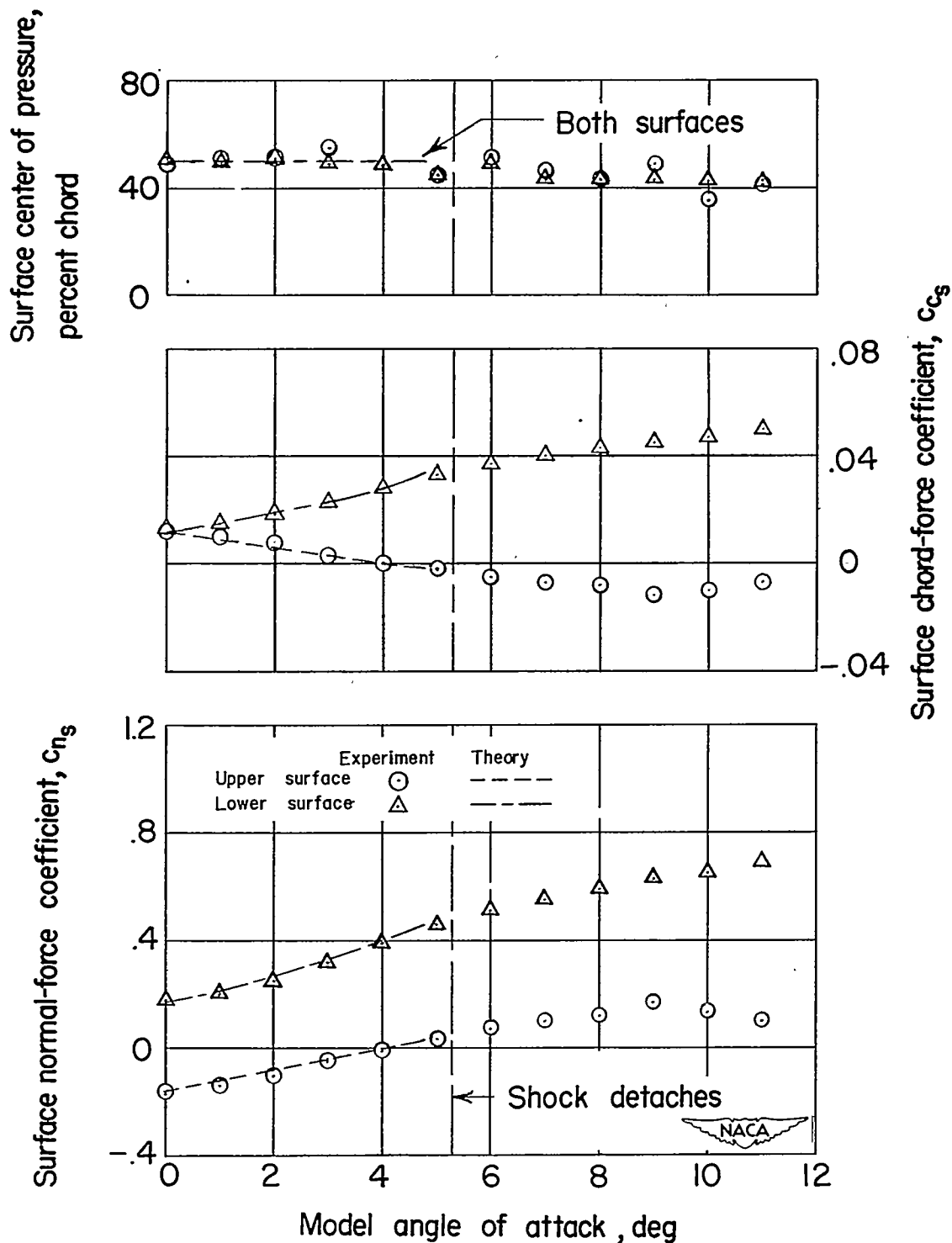stream static pressure.

Figure 9.- Aerodynamic characteristics at the midspan of the upper and
   lower surfaces of an 8.2° wedge of aspect ratio 3.3. M = 1.40. Base
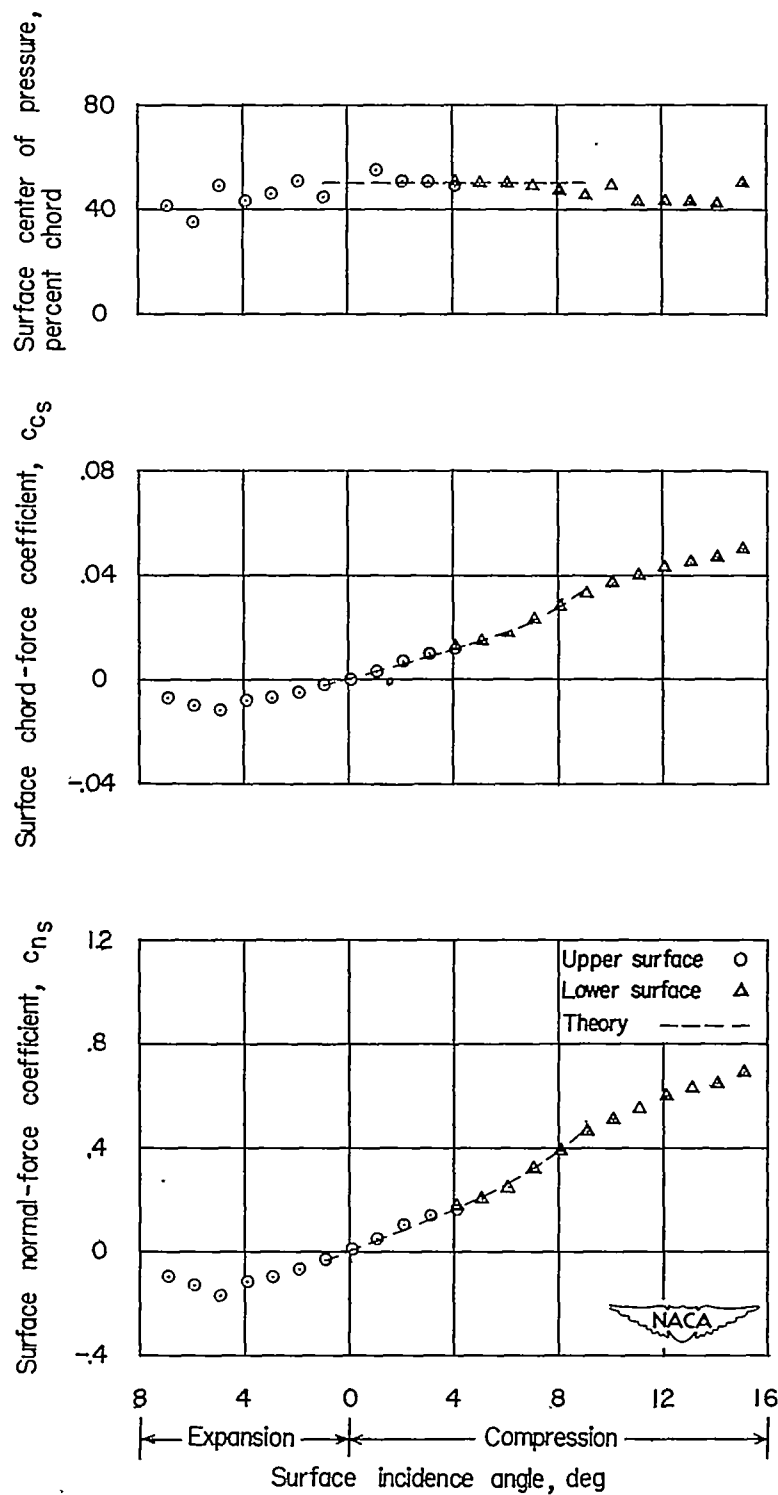   pressure assumed equal to free-stream static pressure.

Figure 10.- Expansion and compression surface midspan aerodynamic coefficients. Aspect ratio, 3.3; M = 1.40. Base pressure assumed equal to free-stream static pressure.